

Laminin $\beta 2$ Gene Missense Mutation Produces Endoplasmic Reticulum Stress in Podocytes

Ying Maggie Chen,* Yuefang Zhou,* Gloriosa Go,* Joseph T. Marmorstein,* Yamato Kikkawa,[†] and Jeffrey H. Miner^{*‡}

*Renal Division and [‡]Department of Cell Biology and Physiology, Washington University School of Medicine, St. Louis, Missouri; and [†]Laboratory of Clinical Biochemistry, Tokyo University of Pharmacy and Life Sciences, Tokyo, Japan

ABSTRACT

Mutations in the laminin $\beta 2$ gene (*LAMB2*) cause Pierson syndrome, a severe congenital nephrotic syndrome with ocular and neurologic defects. *LAMB2* is a component of the laminin-521 ($\alpha 5\beta 2\gamma 1$) trimer, an important constituent of the glomerular basement membrane (GBM). The C321R-*LAMB2* missense mutation leads to congenital nephrotic syndrome but only mild extrarenal symptoms; the mechanisms underlying the development of proteinuria with this mutation are unclear. We generated three transgenic mouse lines, in which rat C321R-*LAMB2* replaced mouse *LAMB2* in the GBM. During the first postnatal month, expression of C321R-*LAMB2* attenuated the severe proteinuria exhibited by *Lamb2*^{-/-} mice in a dose-dependent fashion; proteinuria eventually increased, however, leading to renal failure. The C321R mutation caused defective secretion of laminin-521 from podocytes to the GBM accompanied by podocyte endoplasmic reticulum (ER) stress, likely resulting from protein misfolding. Moreover, ER stress preceded the onset of significant proteinuria and was manifested by induction of the ER-initiated apoptotic signal C/EBP homologous protein (CHOP), ER distention, and podocyte injury. Treatment of cells expressing C321R-*LAMB2* with the chemical chaperone taurodeoxycholic acid (TUDCA), which can facilitate protein folding and trafficking, greatly increased the secretion of the mutant *LAMB2*. Taken together, these results suggest that the mild variant of Pierson syndrome caused by the C321R-*LAMB2* mutation may be a prototypical ER storage disease, which may benefit from treatment approaches that target the handling of misfolded proteins.

J Am Soc Nephrol 24: 1223–1233, 2013. doi: 10.1681/ASN.2012121149

Pierson syndrome (Online Mendelian Inheritance in Man #609049), a rare autosomal recessive disease, is characterized by renal failure from congenital nephrotic syndrome/diffuse mesangial sclerosis, severe ocular abnormalities, and neurodevelopmental impairments.^{1–3} Pierson syndrome is caused by mutations in the laminin $\beta 2$ gene (*LAMB2*).⁴

Laminin, type IV collagen, nidogen, and sulfated proteoglycans comprise the glomerular basement membrane (GBM),⁵ an unusually thick BM formed by fusion of distinct BMs assembled by podocytes and glomerular endothelial cells.⁶ Laminins are obligate heterotrimeric glycoproteins containing one α -, one β -, and one γ -chain.⁷ The major laminin heterotrimer in the mature GBM is laminin $\alpha 5\beta 2\gamma 1$ (LM-521).⁸ Laminin trimerization occurs

in the endoplasmic reticulum (ER) and involves association of the three chains along their laminin coiled-coil domains to form the long arm.⁹ After trimers are secreted into the extracellular space, they polymerize with each other to form the supra-molecular laminin network through interactions among the amino-termini of the short arms (laminin amino-terminal [LN] domains).^{10,11} *Lamb2*^{-/-} mice

Received December 4, 2012. Accepted March 12, 2013.

Published online ahead of print. Publication date available at www.jasn.org.

Correspondence: Dr. Jeffrey H. Miner, Washington University School of Medicine, Renal Division 8126, 660 S. Euclid Avenue, St. Louis, MO 63110. Email: minerj@wustl.edu

Copyright © 2013 by the American Society of Nephrology

exhibiting congenital nephrotic syndrome,¹² abnormal neuromuscular junctions,^{13–16} and abnormalities in the retina¹⁷ recapitulate Pierson syndrome.

LAMB2 null mutations cause the full syndromic phenotype of Pierson syndrome, whereas certain *LAMB2* missense mutations, including R246Q, C321R, L1393F, and N1380K, cause congenital nephrotic syndrome with mild extrarenal features.¹⁸ These mild variants of Pierson syndrome have expanded the clinical spectrum of *LAMB2*-associated disorders. We previously showed that defective laminin secretion from podocytes to the GBM underlies the R246Q mutation-caused congenital nephrotic syndrome.¹⁹

Missense mutations can lead to protein misfolding and disruption of protein trafficking.^{20,21} Alterations in protein trafficking occur mainly in the ER, the central site for folding, post-translational modifications, and transport of secretory, luminal, and membrane proteins. Protein folding in the ER is facilitated by ER-resident molecular chaperones and enzymes, such as immunoglobulin binding protein (BiP)/glucose-regulated protein (GRP)78, GRP94, oxygen-regulated protein 150 calnexin, calreticulin, and protein disulfide isomerase.^{22,23} An imbalance between the load of misfolded proteins and the folding capacity of the ER leads to ER stress.²⁴ The ER responds to stress by activating the unfolded protein response (UPR), which is initiated by three ER transmembrane proteins—protein kinase regulated by RNA-like ER kinase, inositol-requiring protein-1, and activating transcription factor-6. BiP/GRP78 is also a key sensor linked to the UPR in stressed cells. Protein kinase regulated by RNA-like ER kinase phosphorylates eukaryotic initiation factor-2, leading to attenuation of protein translation and induction of activating transcription factor-4 and its target CCAAT/enhancer-binding protein homologous protein (CHOP), which is an ER-specific proapoptotic transcription factor.²⁵ Misfolded protein and the resultant ER stress represent one important cause of ER storage diseases, such as cystic fibrosis,²⁶ α 1-antitrypsin deficiency,²⁷ retinitis pigmentosa,²⁸ and Alzheimer's disease.²⁹ Accumulating evidence also suggests that ER stress contributes to the development and progression of kidney disease.³⁰

Here, we investigate the mechanisms by which the C321R-*LAMB2* missense mutation causes nephrotic syndrome using a knockout/transgenic approach to replace endogenous mouse laminin β 2 with different levels of C321R mutant rat β 2 together with an *in vitro* system. Our studies suggest that the C321R mutation impairs secretion of mutant laminin-521 from podocytes, resulting in low GBM laminin levels and altered GBM composition. Our results also indicate that podocyte ER stress and injury are linked to the development of proteinuria and that a chemical chaperone can partially ameliorate the secretion defect *in vitro*. These data advance our understanding of the molecular pathogenesis of *LAMB2* mutation-induced congenital nephrotic syndrome and suggest a strategy for therapeutic intervention in this disease.

RESULTS

Generation and Characterization of Podocyte-Specific Mouse Nephrin Promoter-C321R-*LAMB2* Transgenic Mice

To investigate the mechanisms whereby the C321R-*LAMB2* mutation causes congenital nephrotic syndrome, we generated transgenic mice, in which a full-length rat β 2 cDNA with an engineered C321R mutation was placed under the control of the podocyte-specific mouse nephrin promoter (NEPH). Three individual NEPH-C321R-*LAMB2* transgenes were bred onto the *Lamb2*^{-/-} background. The fact that the expression of the wild-type (WT) rat β 2 cDNA in podocytes through NEPH is sufficient to restore the integrity of the glomerular filtration barrier (GFB) in *Lamb2*^{-/-} mice³¹ is proof of principle that *Lamb2*^{-/-} mice expressing mutant rat β 2 in podocytes serve as useful models for mild variants of Pierson syndrome.

In *Lamb2*^{-/-}; NEPH-C321R-*LAMB2* mice, the endogenous WT mouse β 2 in the GBM was replaced by the mutant C321R-*LAMB2*. Transgene expression was assayed by both quantitative confocal immunofluorescence microscopy^{19,32} and *in situ* hybridization on the *Lamb2*^{-/-} background. As shown in Figure 1A, dual immunostaining of kidney sections for rat laminin β 2 and the GBM marker agrin identified three independent lines of transgenic mice with differing levels of rat β 2 in the GBM (Tg^{Lo}, Tg^{Med}, and Tg^{Hi} represent the low, medium, and high transgene expressors, respectively). It was also noted that the highest C321R expressor (C321R-Tg^{Hi}) exhibited a lower level of β 2 in the GBM than the lowest R246Q expressor (R246Q-Tg^{Lo}) studied previously (Figure 1A). Moreover, as we previously showed,¹⁹ rat β 2 protein levels in the GBM were much higher in *Lamb2*^{-/-} mice expressing WT rat β 2 (*Lamb2*^{-/-}; Tg-WT) than in R246Q-Tg^{Lo} mice (Figure 1B). Surprisingly, transgene-derived mRNA was easily detected by *in situ* hybridization in C321R-Tg^{Med} and -Tg^{Hi} and the Tg-WT kidneys in a podocyte-specific pattern, although not in C321R-Tg^{Lo} or R246Q-Tg^{Lo} kidneys (Figure 1C). Taken together, analysis of transgene-derived mRNA and protein levels suggests that, even with transcription levels comparable with those levels of the WT β 2 transgene in podocytes (and higher than the endogenous mouse *Lamb2* mRNA¹⁹), C321R-*LAMB2* protein levels in the GBM were comparatively very low.

Proteinuria in *Lamb2*^{-/-}; NEPH-C321R-*LAMB2* Mice

Because proteinuria is the most sensitive clinical manifestation of GFB defects, we examined the *in vivo* function of C321R-*LAMB2* mutant protein in the GBM by comparing proteinuria in the three lines of *Lamb2*^{-/-}; NEPH-C321R-*LAMB2* mice with their *Lamb2*^{-/-} and WT littermates. Spot urinary protein to creatinine ratios were determined every 2 weeks for up to 12 weeks. *Lamb2*^{-/-} mice developed severe proteinuria and died by 4–5 weeks. Between 3 and 4 weeks of age, the average protein to creatinine ratios (gram/gram) for *Lamb2*^{-/-} ($n=12$), Tg^{Lo} mutants ($n=10$), Tg^{Med} mutants ($n=9$), Tg^{Hi}

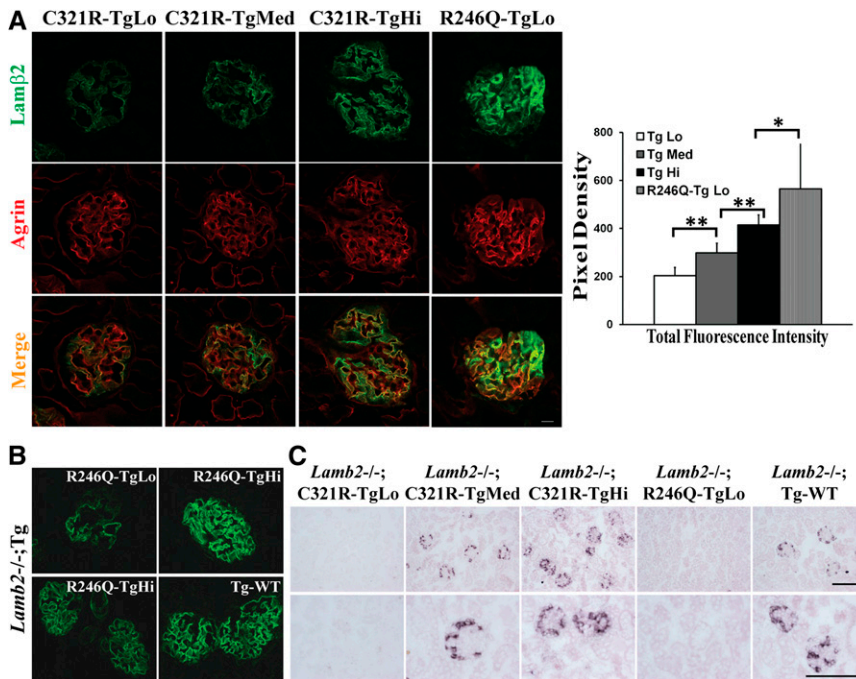


Figure 1. There are three different levels of NEPH-C321R-LAMB2 transgene expression in the three independent lines. These are revealed by (A and B) quantitative confocal immunofluorescence and (C) *in situ* hybridization. Transgenes were on the *Lamb2*^{-/-} background in all cases. (A) Quantitative confocal immunofluorescence showed different levels of transgene-derived rat C321R-LAMB2 and R246Q-LAMB2 proteins in the GBM. LAMB2 protein accumulation in the GBM was detected at ~3 weeks of age by colocalization of mutant LAMB2 (green) and agrin (red) in overlay images (merge). As shown in the histogram, significant differences in total fluorescence intensity were observed in glomeruli of the different groups ($n=20$ – 25 glomeruli for each line). $**P<0.001$, $*P<0.05$ by *t* test. Scale bar, $10\ \mu\text{m}$. (B) Panels from our previous paper¹⁹ show that Tg-WT mice exhibited much higher rat $\beta 2$ in the GBM compared with R246Q-Tg^{Lo} mutants. To avoid image saturation and the resulting quantification errors, different laser intensities and gains were used for the upper and lower panels; R246Q-Tg^{Hi} staining was used as a common reference for comparison between R246Q-Tg^{Lo} mutants and the Tg-WT mice. Original magnification, $\times 800$. (C) Transgene-derived mRNA was easily detected by *in situ* hybridization in C321R-Tg^{Med}, C321R-Tg^{Hi}, and Tg-WT mice but not C321R-Tg^{Lo} or R246Q-Tg^{Lo} mutants (at approximately 3 weeks). Scale bars, $100\ \mu\text{m}$.

mutants ($n=5$), and control WT littermates ($n=47$) were 124.76 ± 54.18 , 73.61 ± 33.49 , 21.5 ± 18.18 , 15.4 ± 4.07 , and 3.99 ± 2.78 , respectively (Figure 2). The differences between Tg^{Lo} or *Lamb2*^{-/-} and any of the other groups were statistically significant ($P<0.001$). Although Tg^{Med} mutants seemed to have developed more proteinuria compared with Tg^{Hi} mutants by 4 weeks, the difference did not reach statistical significance. These data indicate that, in the first postnatal month, the severe proteinuria in *Lamb2*^{-/-} mice was attenuated in a dose-dependent fashion by GBM accumulation of C321R-LAMB2; this result was also associated with prolonged lifespan. However, proteinuria increased in all three lines after the first month (data not shown), leading to renal failure and death by 3 months of age. Nevertheless, these results suggest

that even the lowest expression of C321R-LAMB2 provides significant benefit.

Effects of C321R-LAMB2 on GBM Composition

During glomerulogenesis, there is a transition in laminin deposition, such that the $\alpha 1\beta 1\gamma 1$ and $\alpha 5\beta 1\gamma 1$ trimers are present in the nascent GBM but are replaced by LM-521 as maturation proceeds.^{33,34} In the absence of laminin $\beta 2$, laminin $\beta 1$ persists in the GBM,¹² and laminins $\alpha 1$, $\alpha 2$, $\alpha 3$, $\beta 3$, and $\gamma 2$ are ectopically deposited,³⁵ perhaps as a compensatory response to abnormal GBM that might also be pathogenic. We, therefore, investigated how the replacement of WT LAMB2 with mutant C321R-LAMB2 impacted the laminin composition of the GBM. We examined laminin chain repertoire in Tg^{Hi} mutants at 3 weeks, when proteinuria was minimal. By immunostaining, the normally mesangial laminins $\alpha 1$ and $\alpha 2$ (Figure 3, A and E and Supplemental Figure 1, A and B) were ectopically deposited in the GBMs of Tg^{Hi} (Figure 3, B and F and Supplemental Figure 1, A and B) and non-transgenic *Lamb2*^{-/-} mutants (Figure 3, C and G and Supplemental Figure 1, A and B). In contrast, laminins $\alpha 1$ and $\alpha 2$ were found only in the mesangium of the *Lamb2*^{-/-}; Tg-WT glomeruli (Figure 3, D and H and Supplemental Figure 1, A and B). Additionally, although laminin $\beta 1$ disappeared from the GBM of WT and *Lamb2*^{-/-}; Tg-WT kidneys (Figure 3, I and L and Supplemental Figure 1C), it persisted in the GBM of Tg^{Hi} and *Lamb2*^{-/-} mice, which was evident by the complete overlap of $\beta 1$ and nidogen, a ubiquitous BM marker, in the GBM (Figure 3, J and K and Supplemental Figure 1C). This finding suggests that high-level podocyte expression of WT $\beta 2$ suppresses ectopic deposition of laminins $\alpha 1$, $\alpha 2$, and $\beta 1$ in the GBM, whereas the reduced level of C321R-LAMB2 and absence of $\beta 2$ in the GBM are associated with accumulation of these potentially pathogenic laminins, which may contribute to the progression of proteinuria.

Histologic and Ultrastructural Features at Early and Later Stages

Light and transmission electron microscopy (TEM) were used to examine renal histopathology in the three lines of *Lamb2*^{-/-}; NEPH-C321R-LAMB2 mice and their WT and *Lamb2*^{-/-} littermates. *Lamb2*^{-/-} mice had developed severe proteinuria by 3 weeks, which was associated with mesangial matrix (MM) expansion and glomerulosclerosis (Figure 4A, d) compared with

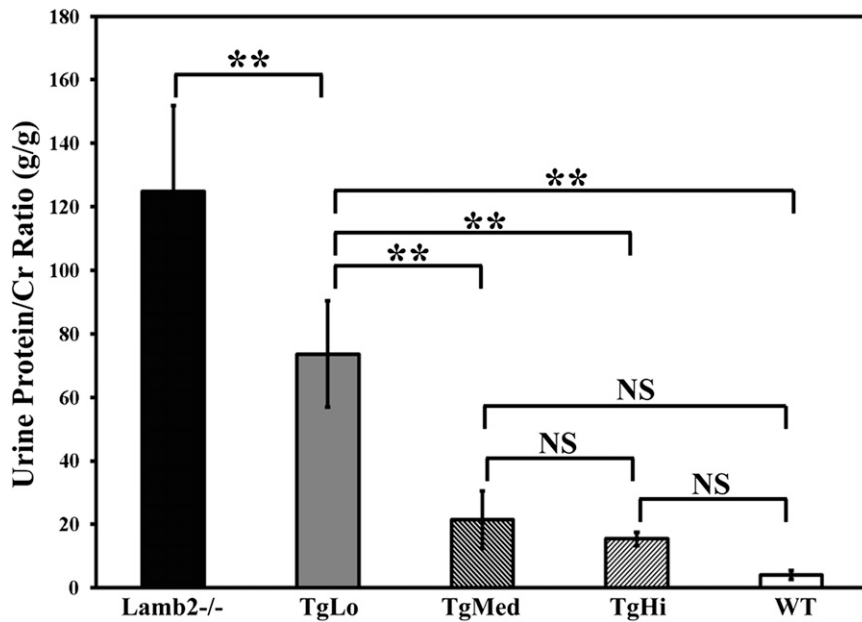


Figure 2. Proteinuria in *Lamb2*^{-/-}; NEPH-C321R-LAMB2 mutant mice correlates inversely with the level of transgene expression before the first month of age. Urinary protein/creatinine ratios (gram/gram) between 3 and 4 weeks of age in the three lines of *Lamb2*^{-/-}; C321R-LAMB2 mice and their WT and nontransgenic *Lamb2*^{-/-} littermates are shown in the graph as mean ± SD. ***P*<0.001. NS, not significant. Statistical analysis was done by ANOVA with the Tukey multiple comparison test.

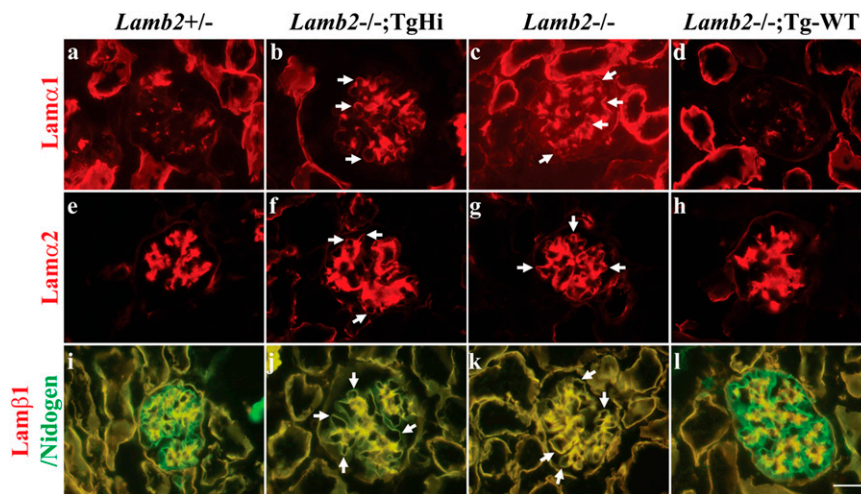


Figure 3. Ectopic deposition of laminins $\alpha 1$, $\alpha 2$, and $\beta 1$ in the GBM is associated with reduced expression of $\beta 2$ in the GBM of *Lamb2*^{-/-}; C321R-LAMB2 mice. Frozen kidney sections from Tg^{Hi} mutants, their WT and nontransgenic *Lamb2*^{-/-} littermates, and age-matched *Lamb2*^{-/-}; Tg-WT mice were stained for laminin chains at 3 weeks. (A and E) The normally mesangial laminins $\alpha 1$ and $\alpha 2$ were ectopically deposited in the (B and F, arrows) Tg^{Hi} and (C and G, arrows) *Lamb2*^{-/-} GBM but not (D and H) Tg-WT GBM. I–L show merged images for which overlapping laminin $\beta 1$ (red) and nidogen (green) signals appear (J and K, arrows) yellow in the GBM of *Lamb2*^{-/-}; Tg^{Hi} and *Lamb2*^{-/-} mice as well as (I–L) the mesangium of all mice, where both proteins are normally present. Additional data are shown in Supplemental Figure 1. Scale bar, 20 μ m.

controls (Figure 4A, a). Light microscopic examination of hematoxylin and eosin (H&E)-stained kidney sections also revealed diffuse MM expansion in Tg^{Lo} mutants (Figure 4A, b). In contrast, there were no obvious renal histopathological changes in Tg^{Hi} mutants at 3 weeks (Figure 4A, c). Tg^{Med} mutants showed limited glomerulosclerosis (data not shown). Periodic acid–Schiff (PAS) staining at 3 weeks showed that *Lamb2*^{-/-} mice exhibited abundant renal tubular protein casts and complete loss of brush borders in their proximal tubules (Figure 4A, h). Tg^{Lo} mutants showed fewer protein casts and only partial loss of brush borders (Figure 4A, f). In contrast to the above findings, in both Tg^{Med} and Tg^{Hi} mutants, tubular protein casts were rarely seen, and tubular brush borders were preserved (Figure 4A, g) (data not shown).

Ultrastructural analysis revealed diffuse foot process (FP) effacement and mild GBM thickening in 3-week-old *Lamb2*^{-/-} mice (Figure 4B, e). However, although some FP effacement was observed in most glomeruli of the transgenic mutants (Figure 4B, b–d), there were still focal areas with much less severe FP effacement in all three lines at 3 weeks (Figure 4B, f–h), which is consistent with the lower proteinuria compared with their nontransgenic *Lamb2*^{-/-} littermates. There was no significant GBM thickening in the C321R mutants at 3 weeks (Figure 4B, b–d and f–h); however, a moth-eaten appearance of the GBM was sometimes observed in Tg^{Lo} (Figure 4B, b) and Tg^{Med} (Figure 4B, c) mutants but not Tg^{Hi} mutants (Figure 4B, d). These findings suggest that the increased transgene expression and the subsequent increased deposition of C321R-LAMB2 in the GBM partly ameliorate the severe GFB defect in *Lamb2*^{-/-} mice in a dose-dependent manner.

By 6 weeks of age, the three lines of transgenic mutants had developed more severe proteinuria and MM expansion (data not shown). TEM analysis showed diffuse FP effacement and mild GBM thickening in all three lines (Figure 5). In addition, there was more severe interstitial fibrosis in Tg^{Lo} mutants compared with Tg^{Med} and Tg^{Hi} mutants, which was shown by Gomori's Trichrome staining (Figure 5). In summary, consistent with the proteinuria profile (Figure 2), these results at early and later stages

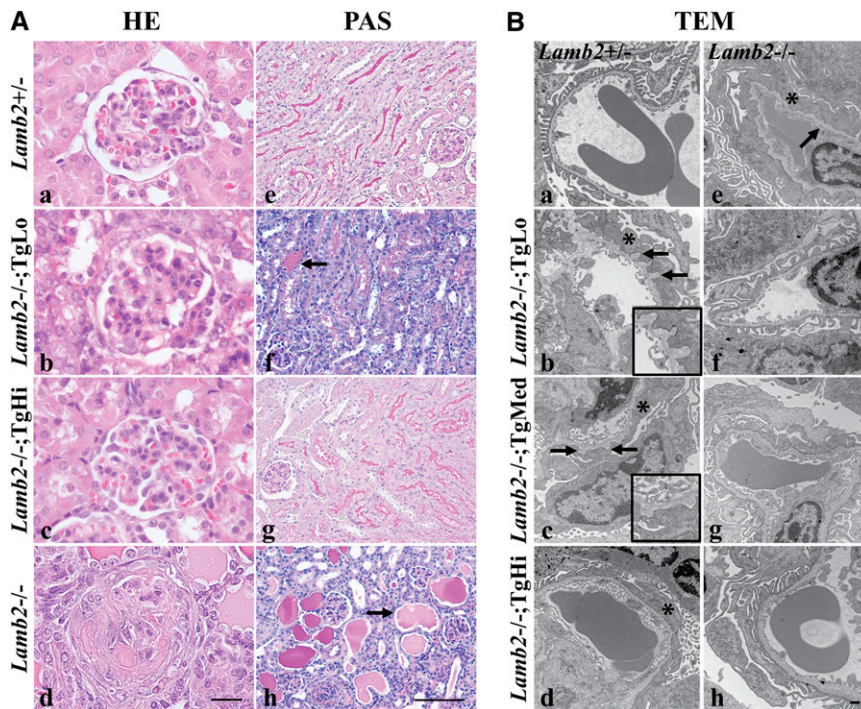


Figure 4. Light and electron microscopy analyses of kidneys from the three lines of *Lamb2*^{-/-}; NEPH-C321R-LAMB2 mice and their *Lamb2*^{-/-} and WT littermates at 3 weeks show that glomerulosclerosis and mild GBM thickening in *Lamb2*^{-/-} mice are attenuated by increased expression of C321R-LAMB2 in the GBM. (A) Paraffin sections of WT and mutant kidneys were stained with H&E (HE) and PAS. *Lamb2*^{-/-} mice showed (d) glomerulosclerosis, (h, arrow) prominent renal tubular protein casts, and (h) loss of brush borders compared with (a and e) the WT littermates. Tg^{Lo} *Lamb2*^{-/-}; C321R-LAMB2 mice exhibited (b) MM expansion, (f, arrow) fewer protein casts, and (f) partial loss of brush borders. (c and g) No obvious pathology was detected in Tg^{Hi} mutants. Scale bars, 20 μ m in a–d; 100 μ m in e–h. (B) TEM showed diffuse FP effacement (*) and mild GBM thickening (arrow) in (e) *Lamb2*^{-/-} mice compared with (a) controls. FP effacement (*) was observed in (b–d) all mutant lines, with some GBM outpocketing in the (b, arrows) Tg^{Lo} and (c, arrows) Tg^{Med} mutants. Insets in b and c magnify regions between the two arrows. (f–h) Focal areas with intact foot processes were also found in the three mutant Tg lines. Scale bar, 500 nm.

of nephrotic syndrome indicate that increased accumulation of C321R-LAMB2 in the GBM correlates with improvements in GFB ultrastructure and kidney histopathological features.

Defective Secretion of C321R-LAMB2-Containing Trimers from Podocytes to the GBM and Induction of Podocyte ER Stress

The fact that a high level of mutant β 2 transcription in podocytes was associated with a low level of β 2 protein in the GBM (Figure 1) suggests that secretion of the mutant from podocytes may be defective. To test this hypothesis, we established stable human embryonic kidney 293T (HEK293T) cell lines expressing fusion proteins, in which the LN domain and laminin epidermal growth factor-like domain a (LEa) of rat WT or C321R β 2 were fused to *Gaussia* luciferase (Gluc), the brightest known luciferase. Secretion of the LAMB2-LN/LEa-Gluc

fusion proteins was directed by the β 2 signal peptide, and trafficking of the fusion proteins was analyzed. Cells were cultured for 48 hours, and media were collected for both Western blot analysis with an anti-Gluc antibody and luciferase assay. Although the WT fusion protein was detected in the medium, the mutant fusion protein was not (Figure 6A). Similarly, the luciferase activity in the medium was significantly higher in the WT-transfected cells compared with the mutant-transfected cells (Figure 6B). In contrast, when cell lysates were subjected to Western blot analysis using the anti-Gluc antibody, both WT and mutant laminin β 2 fusion proteins were easily detected, and the mutant seemed to be more abundant (Figure 6C). Quantitative RT-PCR analysis showed similar *Lamb2* transcript levels in the WT and C321R clones (Figure 6D). Together, these *in vitro* studies directly show that the C321R mutation inhibits secretion of the C321R mutant protein, leading to its intracellular accumulation.

To delineate the subcellular localization of the WT and mutant proteins, stable 293T-Gluc cells were subjected to confocal immunofluorescence staining using antibodies against Gluc and protein disulfide isomerase A3 (PDIA3), an ER resident foldase catalyzing disulfide bond formation and an ER stress marker. Although C321R/Gluc overlapped exclusively with PDIA3 (Figure 6E, b, d, and f), WT/Gluc showed only a partial overlap with PDIA3 (Figure 6E, a, c, and e). This result suggests that the WT/Gluc fusion protein was able to exit the ER and proceed through the secretory pathway, whereas C321R/Gluc was retained inside the ER. In addition, the upregulation of PDIA3 in cells expressing the mutant (Figure 6E, c and d) suggests that C321R/Gluc is misfolded and has triggered ER stress.

We next examined if BiP, an important ER molecular chaperone and a central sensor for the increased load of misfolded proteins, was induced. Western blot analysis showed increased expression of BiP in C321R cells versus WT cells; treatments with tunicamycin, which blocks N-linked glycosylation in the ER and causes ER stress,³⁶ were included as positive controls (Figure 6F). Similarly, double immunofluorescence staining of BiP and the podocyte nucleus marker WT-1 showed a very low level of constitutive expression of BiP in the podocytes of WT and *Lamb2*^{-/-}; Tg-WT mice (Figure 6G, a, e, and i and Figure 6G, b, f, and j, respectively). In contrast, even at 3 weeks, when Tg^{Hi} mutants had developed only trace proteinuria, Tg^{Hi} podocytes

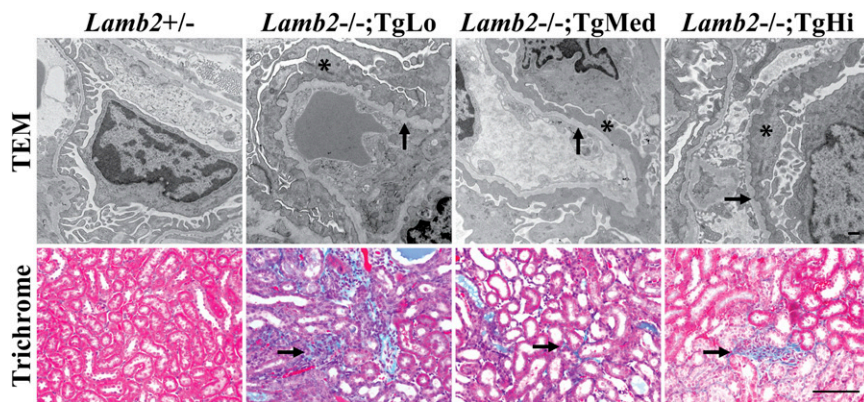


Figure 5. Increased level of C321R-LAMB2 in the GBM is associated with less interstitial fibrosis at 6 weeks. TEM analysis showed irregular GBM thickening (arrows) and diffuse FP effacement (*) in Tg^{Lo}, Tg^{Med}, and Tg^{Hi} *Lamb2*^{-/-}; C321R-LAMB2 mice. Scale bar, 500 nm. Gomori's Trichrome staining revealed less interstitial fibrosis in Tg^{Med} and Tg^{Hi} mutants compared with Tg^{Lo} mutants (arrows). Scale bar, 100 μ m.

exhibited BiP upregulation in all glomeruli (Figure 6G, c, g, and k). Interestingly, significant BiP induction was also observed in the podocytes of 5%–10% of *Lamb2*^{-/-} glomeruli at 3 weeks, when proteinuria was nephrotic range (Figure 6G, d, h, and l). In summary, our *in vitro* and *in vivo* data clearly suggest that the C321R mutation causes protein misfolding, which leads to podocyte ER stress. The fact that induction of BiP in podocytes of Tg^{Hi} mutants with minimal proteinuria was observed in all glomeruli, which is in contrast to the limited increase of BiP in *Lamb2*^{-/-} mice with heavy proteinuria (only seen in 5%–10% of glomeruli), supports the concept that the primary cause of podocyte ER stress is the misfolded C321R-LAMB2 protein rather than proteinuria.

Podocyte ER Distention, CHOP Activation, and Associated Podocyte Injury

ER stress triggers both survival and apoptotic signals. If the UPR is unable to resolve protein folding defects, ER dysfunction can lead to apoptosis.³⁷ We investigated whether induction of ER stress in podocytes led to ER morphologic changes by TEM examination. At 3 weeks, we observed significant podocyte rough ER (rER) distention in Tg^{Hi} mutants (Figure 7A, b) and a prominent vesiculated rER in the podocytes of *Lamb2*^{-/-} littermates (Figure 7A, c). In contrast, *Lamb2*^{-/-}; Tg-WT mice did not show significant podocyte rER dilation (Figure 7A, a).

Chronic and persistent ER stress may activate cell apoptosis by induction of CHOP, a proapoptotic transcription factor specifically related to ER stress. Indeed, at 3 weeks, a marked induction of CHOP was detected in the podocytes of some glomeruli of Tg^{Hi} mutants (Figure 7B, b, e, and h) and *Lamb2*^{-/-} mice (Figure 7B, c, f, and i) versus the Tg-WT mice (Figure 7B, a, d, and g). Moreover, compared with the Tg-WT podocytes (Figure 7C, a, d, and g), there was desmin expression in some podocytes (an indicator of podocyte injury) of the mildly proteinuric Tg^{Hi} mutants (Figure 7C, b, e, and h) and much stronger desmin expression in the podocytes of heavily

proteinuric *Lamb2*^{-/-} mice (Figure 7C, c, f, and i). Collectively, these data suggest that podocyte ER dysfunction, manifested by ER distention and upregulation of CHOP, and the associated podocyte injury caused by the misfolded protein precede the occurrence of significant proteinuria in the Tg^{Hi} mutants. These results also indicate that misfolding of the mutant protein, rather than simply overexpression of any LAMB2 protein (WT or mutant) in podocytes, induces all the above-mentioned events. Associated podocyte ER stress in *Lamb2*^{-/-} mice with heavy proteinuria is perhaps from albumin overload inside *Lamb2*^{-/-} podocytes; indeed, it has been shown that increased albumin endocytosis in cultured podocytes can induce ER stress and apoptosis.³⁸

A Chemical Chaperone Promotes Secretion of Mutant C321R-LAMB2 Protein

Chemical chaperones, such as taurodeoxycholic acid (TUDCA), can assist protein folding in the ER and facilitate the trafficking of mutant proteins. To determine whether chemical chaperones can improve secretion of the mutant C321R protein, 293T cells expressing either the WT/Gluc or the C321R/Gluc fusion protein were incubated with 1 mM TUDCA or vehicle, and the luciferase activity in the medium was determined. TUDCA selectively enhanced secretion of the mutant (Figure 8B) but not the WT fusion protein (Figure 8A) into the medium. These data suggest that TUDCA could be a good therapeutic candidate for the treatment of proteinuria in patients carrying the C321R and perhaps, other missense *LAMB2* mutations.

DISCUSSION

In contrast to the typical Pierson syndrome phenotype, which has been associated primarily with null mutations in *LAMB2*,^{1,4} missense mutations, such as R246Q and C321R, cause mild variants of Pierson syndrome, in which congenital nephrotic syndrome is the predominant manifestation and extrarenal features are less pronounced.¹⁸ *LAMB2* missense mutation is one of the most common disease-causing mutations in early onset nephrotic syndrome.³⁹ Previously, we investigated the mechanisms whereby the R246Q mutation causes congenital nephrotic syndrome¹⁹; here, we determined how the C321R mutation causes proteinuria.

Our results suggest that the mechanisms responsible for nephrotic syndrome in patients harboring the C321R-LAMB2 mutation involve both severely impaired laminin secretion and concomitant podocyte ER stress-associated injury. Our hypothesis is supported by both *in vivo* and *in vitro* data. *In vivo*, we generated three lines of transgenic mice, in which

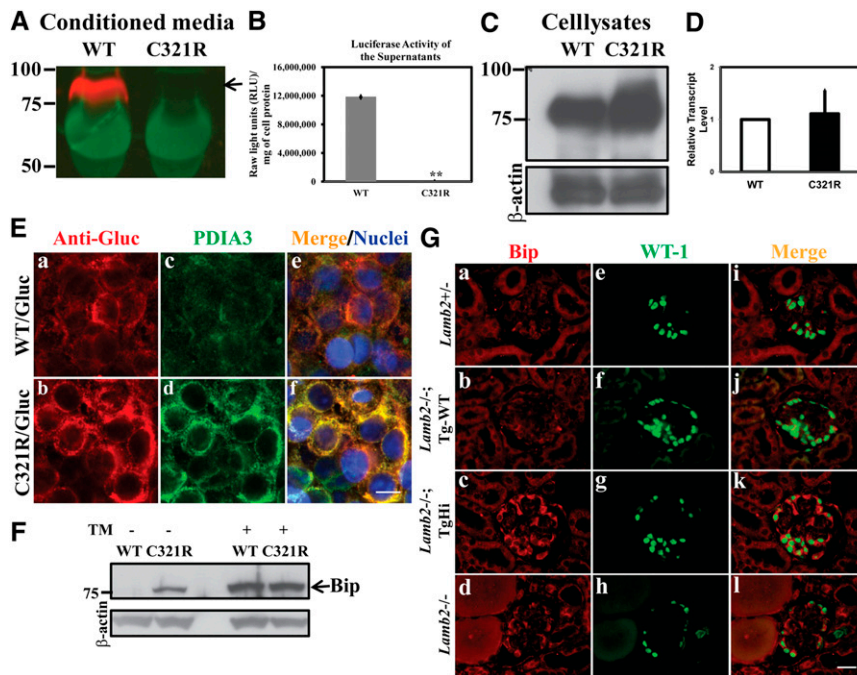


Figure 6. Secretion of the mutant laminin $\beta 2$ fragment/Gluc fusion protein is inhibited and podocyte ER stress is induced in $Tg^{Hi} Lamb2^{-/-}$; C321R-LAMB2 mice. (A, arrow) The WT but not the C321R-LAMB2/Gluc fusion protein was secreted from stably transfected HEK293T cells. (B) This finding was reflected by luciferase activity in the media (** $P < 0.001$ by t test). The data are presented as mean \pm SD of three independent media samples. (C) The C321R/Gluc fusion protein was retained intracellularly compared with the WT fusion protein. (D) Quantitative RT-PCR did not show a significant difference in $Lamb2$ mRNA levels between the WT and C321R cell clones. Data are presented as mean \pm SD of fold changes of four independent samples from each clone. $P > 0.05$ by t test. (E) Colocalization of the (a) WT/Gluc or (b) C321R LAMB2/Gluc fusion protein with the (c and d) ER marker PDIA3 in the 293T-Gluc cells using confocal microscopy. (e and f) Nuclei were counterstained with Hoechst 33342 (blue). (a, c, and e) The WT fusion protein seemed to be transiently associated with PDIA3, but (b, d, and f) the mutant was completely colocalized with PDIA3, indicating accumulation in the ER. (c and d) The mutant protein also induced expression of PDIA3. Scale bar, 10 μm . (F) Cell lysates of 293T-Gluc clones were subjected to Western blot analysis. The C321R but not the WT fusion protein increased BiP expression (arrow). Tunicamycin (TM) -treated cells served as positive controls. (G) Frozen kidney sections from mice of the indicated genotypes were examined by dual immunofluorescence staining of BiP and WT-1 at 3 weeks. Compared with the very low level expression of (a, e, and i) BiP in the control podocytes, BiP upregulation was detected in podocytes of (c, g, and k) Tg^{Hi} glomeruli and (d, h, and l) some $Lamb2^{-/-}$ glomeruli but not (b, f, and j) podocytes of Tg-WT glomeruli. Scale bar, 20 μm .

C321R-LAMB2 mRNA was expressed in podocytes at differing levels, two of which were comparable with the expression level of the WT $\beta 2$ transgene. Our analysis revealed that ample levels of C321R-LAMB2 mRNA in podocytes were associated with unexpectedly low levels of C321R-LAMB2 protein in the GBM, suggesting a secretion defect. *In vitro*, biochemical studies confirmed that secretion of C321R-LAMB2 was severely inhibited compared with WT-LAMB2. Moreover, the fact that podocyte desmin activation and FP effacement preceded overt proteinuria in the C321R mutant indicates that a primary podocyte injury is also crucial in the development of

proteinuria. The mutant C321R-LAMB2 protein induced podocyte ER stress, which was indicated by the upregulation of the ER chaperones PDIA3 and BiP. Failure to relieve sustained and excessive ER stress led to podocyte injury, which was associated with activation of the ER stress-mediated apoptotic signal CHOP and ER dilation and dysfunction. In addition, the fact that the accumulation of ectopic laminins $\alpha 1$, $\alpha 2$, and $\beta 1$ in the GBM occurred before marked proteinuria suggests another possible mechanism to accelerate the progression of proteinuria, which is most likely secondary to the reduced level of LM-521 in the GBM.

An important caveat here is that we did not find accumulation of C321R-LAMB2 protein inside podocytes because of deficient secretion. It is known that ER quality control mechanisms include ER-associated degradation (ERAD), and induction of the UPR may increase ERAD capacity. Thus, the bulk of the misfolded C321R-LAMB2 that is not secreted into the GBM may be degraded by ERAD rapidly and become depleted. The $\Delta F508$ mutation in the cystic fibrosis transmembrane conductance regulator⁴⁰ and missense mutations of Wolfram syndrome gene 1 in Wolfram syndrome⁴¹ are other prominent examples of functional proteins that are retained in the ER and degraded by ERAD. Our findings in mice suggest that the mild variant of Pierson syndrome caused by the C321R mutation may be a prototypical ER storage disease, in which the missense mutation leads to a recessive loss-of-function state. The autosomal recessive pattern of inheritance in the mild variants of Pierson syndrome is in agreement with this hypothesis. The aberrantly folded $\beta 2$ protein may be retrotranslocated into the cytoplasm, tagged by ubiquitin ligase, and degraded by the 26S proteasome. However, it is also possible that the misfolded protein is degraded by the lysosome-autophagy pathway coupled with ER stress. Additional studies will be aimed at investigating the mechanisms of mutant protein degradation.

Protein overexpression can also induce ER stress. To ensure that the identified podocyte ER stress response and ER distention are not caused by transgene overexpression, $Lamb2^{-/-}$ mice expressing WT rat $\beta 2$ ($Lamb2^{-/-}$; Tg-WT) were included as important controls in the relevant experiments. Our data clearly show that protein misfolding, but not overexpression, causes ER stress. At a molecular level, the mutation of Cys 321 to

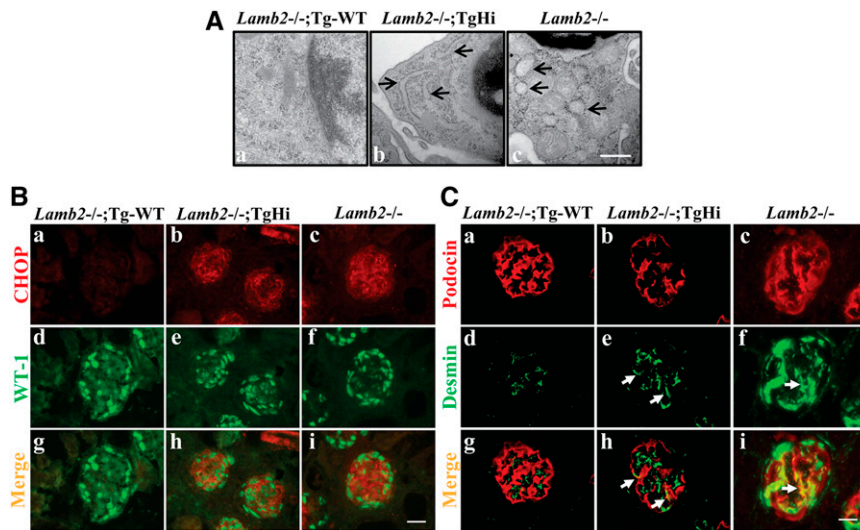


Figure 7. C321R-LAMB2 causes podocyte ER distention, upregulation of CHOP, and activation of desmin in podocytes at 3 weeks. (A) TEM showed that rER in the podocytes of (b, arrows) Tg^{Hi} *Lamb2*^{-/-}; C321R-LAMB2 and (c, arrows) *Lamb2*^{-/-} mice was dilated compared with rER in the (a) podocytes of age-matched *Lamb2*^{-/-}; Tg-WT controls. The swollen, ribosome-studded (b, arrows) tubular structures or (c, arrows) vesicles identify the rER. Scale bar, 500 nm. (B) Double immunofluorescence staining for (a–c) CHOP and (d–f) WT-1 on frozen kidney sections revealed podocyte induction of CHOP in (b, e, and h) *Lamb2*^{-/-}; Tg^{Hi} and (c, f, and i) *Lamb2*^{-/-} glomeruli but not (a, d, and g) Tg-WT glomeruli. Scale bar, 20 μ m. (C) Frozen sections of *Lamb2*^{-/-}; Tg-WT, *Lamb2*^{-/-}; Tg^{Hi}, and *Lamb2*^{-/-} kidneys were stained for (a–c) podocin and (d–f) desmin and (g–i) merged. Compared with (a, d, and g) controls, desmin expression was activated in the podocytes of (b, e, and h, arrows) mildly proteinuric Tg^{Hi} mutants and (c, f, and i, arrows) highly proteinuric *Lamb2*^{-/-} mutants. Scale bar, 20 μ m.

Arg must disrupt disulfide bonding in the LEa domain, which contains multiple EGF-like repeats that each include eight disulfide-bonded cysteines, and this disruption could easily result in LAMB2 misfolding.

Chemical chaperones can stabilize protein conformation and rescue trafficking-defective but otherwise functional misfolded proteins.⁴² They have been used in the treatment of cystic fibrosis,^{26,43} α 1-antitrypsin deficiency,⁴⁴ nephrogenic diabetes insipidus,⁴⁵ Gaucher's disease,⁴⁶ and Fabry's disease⁴⁷ *in vitro* or in animal models. We have shown here that increased accumulation of the C321R mutant protein in the GBM alleviates proteinuria, and TUDCA partially rescues the secretion defect of the mutant protein *in vitro*. Attempts to test TUDCA and other chemical chaperones in our animal model are in progress. Considering that the mutant protein may be degraded, an alternative strategy of combining a proteasome or lysosome inhibitor with a chemical chaperone may be required.

CONCISE METHODS

Generation of Mutant Rat Laminin β 2 Transgenic Mice

Site-directed mutagenesis of the rat *Lamb2* cDNA, construction of the NEPH-C321R-LAMB2 transgene, and production and identification

of transgenic mice were performed as described previously.^{19,31} All animal experiments conformed to the National Institutes of Health Guide for the Care and Use of Laboratory Animals and were approved by the Washington University Animal Studies Committee.

Antibodies, Immunofluorescence, and *In Situ* Hybridization

Commercially available antibodies were obtained as follows: mouse anti-rat laminin β 2 carboxy-terminal coiled-coil domain mAbs D5 and D7⁴⁸ were from the Developmental Studies Hybridoma Bank (Iowa City, IA); rabbit anti-mouse agrin laminin globular domains⁴⁹ were from Takako Sasaki (University of Erlangen-Nürnberg, Erlangen, Germany); rat anti-mouse laminin α 2 mAb 4H8–2 was from Enzo Life-sciences (Farmingdale, NY); mouse IgG1 anti-human desmin clone D33, which crossreacts with mouse desmin, was from DAKO (Carpinteria, CA); rat anti-mouse nidogen clone ELM1 was from Millipore (Billerica, MA); rabbit anti-mouse BiP and CHOP antibodies were from Santa Cruz (Santa Cruz, CA); and mouse IgG1 anti-mouse WT-1 antibody was from Thermo Scientific (Kalamazoo, MI). Other primary antibodies were gifts from generous colleagues: rat anti-mouse laminin α 1 mAb 8B3⁵⁰ was from Dale Abrahamson (University of Kansas Medical Center, Kansas City, KS); rabbit anti-mouse

laminin β 1⁵¹ was from Takako Sasaki (University of Erlangen-Nürnberg, Erlangen, Germany); and rabbit anti-mouse podocin was from Corinne Antignac (Necker Hospital, Paris, France). Alexa 488- and Alexa 594-conjugated secondary antibodies were purchased from Invitrogen (Carlsbad, CA).

Immunofluorescence staining on frozen sections was performed as described previously.³¹ For CHOP staining, frozen sections were fixed with 4% paraformaldehyde in PBS for 10 minutes and permeabilized with 1% Triton X-100 for 5 minutes at room temperature. For BiP staining, kidneys were fixed by transcardiac perfusion with PBS containing 4% paraformaldehyde, and paraffin-embedded sections were used. After dewaxing, the antigen was retrieved by BD Retrieval Solution (BD Pharmingen, San Jose, CA) for 10 minutes at 89°C and permeabilized with 1% Triton X-100 for 5 minutes at room temperature. For immunocytochemistry, 293T-Gluc cells were seeded on coverslips coated with 5 μ g/ml rat collagen I dissolved in 0.02 M acetic acid in 24-well plates for 48 hours. The cells were fixed with ice-cold acetone for 10 minutes at -20° C and blocked with 1% BSA and 1% normal goat serum for 1 hour at room temperature followed by incubation with rabbit anti-Gluc (New England Biolabs, Ipswich, MA) and mouse IgG1 anti-human PDIA3 (Abnova, Walnut, CA) antibodies for an additional 1 hour at room temperature. The coverslips were washed with PBS and incubated with the corresponding Alexa 488- or 594-conjugated secondary antibodies and Hoechst

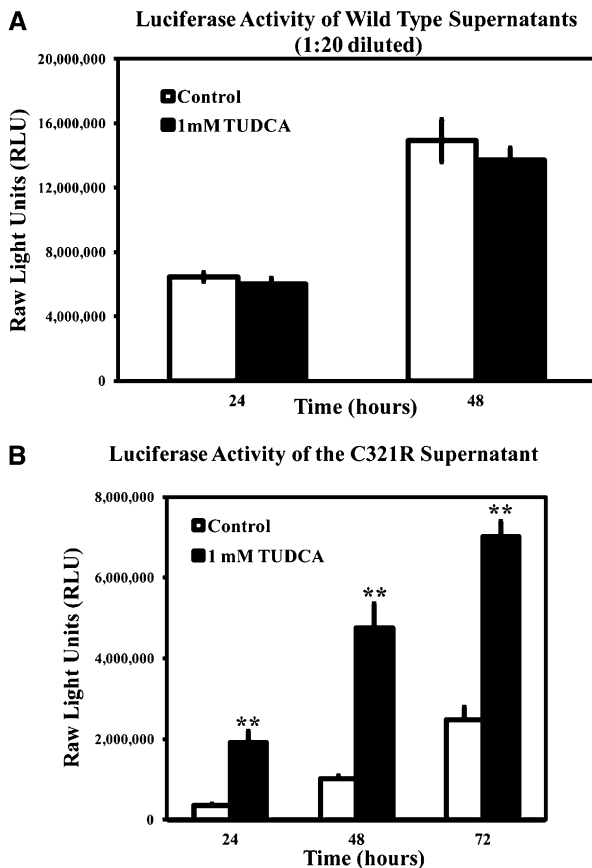


Figure 8. TUDCA treatment increases secretion of the C321R-LAMB2/Gluc fusion protein *in vitro*. Secretion of (A) WT or (B) C321R mutant $\beta 2$ fragment/Gluc fusion proteins from stably transfected 293T cells was measured by luciferase assays at different time points. The data are presented as mean \pm SD of three independent media samples at 24, 48, or 72 hours. (A) TUDCA did not affect secretion of the WT fusion protein ($P > 0.05$ by t test). (B) Secretion of the C321R fusion protein was enhanced by the addition of 1 mM TUDCA from 24 to 72 hours (** $P < 0.001$ by t test). Note that the medium assayed in A was diluted 1:20.

33342 to stain nuclei. The coverslips were then mounted with anti-quench solution and visualized using a Nikon TE-2000 confocal microscopy (Melville, NY).

In situ hybridization was performed as previously described¹⁹ using 1 ng/ μ l cRNA probe. After hybridization, sections were mounted in Crystal/Mount (Biomedica, Foster City, CA).

Confocal Microscopy and Quantitative Image Analysis

Confocal microscopy was used to quantify the levels of laminin $\beta 2$ accumulation in the GBM in the three C321R and the one R246Q mutant $\beta 2$ transgenic lines. In the individual comparative studies, 8- μ m kidney cryosections of the different genotypes were placed on the same slide and immunolabeled with the same mixture of primary antibodies (D5 and D7) and Alexa 488-conjugated secondary antibody. The slides were then examined under a Nikon TE-2000 scanning laser confocal microscope (Melville, NY), and Z-series images

were captured at 0.3- μ m intervals. For each genotype, 20–25 glomeruli were scanned, and the images were captured on the same day using the same laser intensity, confocal aperture, and gain. Raw confocal images taken from the mid-regions of the glomeruli were imported into Image J software. Total pixel density within a fixed circle, which was slightly smaller than the smallest glomerular field, was used to measure glomerular immunofluorescence intensity. The mean intensity for each genotype was compared statistically using a t test.

Light and Electron Microscopy

For light microscopy, kidneys were fixed in 10% buffered formalin, dehydrated through graded ethanols, embedded in paraffin, sectioned at 4 μ m, and stained with H&E, PAS, and Gomori's Trichrome by standard methods. For TEM, tissues were fixed, embedded in plastic, sectioned, and stained as described previously.¹²

Establishment of Stable 293T Cells Expressing Gluc-Tagged Laminin $\beta 2$ Fragments

We used a mammalian expression vector, pCMV-Gluc (New England Biolabs), containing a recombinant Gluc-Tag to which WT and site-directed mutant rat laminin $\beta 2$ fragments containing the LN and LEa domains were fused. The expression constructs were transfected into HEK293T cells in 24-well plates using Lipofectamine 2000 (Invitrogen). Individual clones were isolated, and stable transfectants were selected in medium containing 25 μ g/ml Zeocin (Invitrogen). Established clones were maintained in DMEM (Gibco, Grand Island, NY) supplemented with 10% heat-inactivated FBS (Gibco) and 25 μ g/ml Zeocin.

Western Blot Analysis

Stable 293T-Gluc cells were cultured for 48 hours. Cells were lysed by RIPA buffer (Sigma) containing protease inhibitor cocktail (Roche, Indianapolis, IN), and the protein concentration of each cell lysate was determined by Bio-Rad protein assay (Hercules, CA) using BSA as a standard. Denatured proteins were separated on polyacrylamide gels and then transferred to polyvinylidene difluoride membranes. Blots were blocked with 5% nonfat milk for 1 hour and then incubated overnight with primary antibodies. The membranes were washed with Tris-buffered saline/Tween buffer and incubated with the appropriate horseradish peroxidase-conjugated secondary antibody. The proteins were then visualized in an x-ray developer using ECL-plus detection reagents (GE, Pittsburgh, PA). To ensure equal protein loading, the same blot was stripped with stripping buffer (25 mM glycine + 1% SDS, pH=2.0) and then incubated with a horseradish peroxidase-conjugated mouse anti-human β -actin antibody (Sigma). To examine secretion of LAMB2/Gluc fusion proteins, 40 μ l conditioned media were subjected to Western blot analysis with a fluorescence-conjugated (IRDye 680LT) goat anti-rabbit secondary antibody (Li-Cor Biosciences, Lincoln, NE) and visualized in an infrared imaging system (Li-Cor Biosciences). Rabbit anti-Gluc antibody was from New England Biolabs.

Luciferase Assay

The Gluc activity in the media of 293T-Gluc cells stably expressing either WT or mutant LAMB2/Gluc was assayed by a BioLux Gaussia Luciferase Assay Kit (New England Biolabs) according to the manufacturer's

instructions and quantified with a Femtomaster FB12 Luminometer (Zylux, Oak Ridge, TN). The actual values of raw light units were normalized with respect to total cell protein for each group.

mRNA Quantification by Real-Time PCR

Total RNA from the individual WT and mutant 293T-Gluc clones was extracted using the RNeasy kit (QIAGEN, Valencia, CA) with subsequent DNaseI treatment; 1 μ g RNA was then reverse-transcribed using an RT-PCR Kit (Superscript III; Invitrogen). mRNAs of the WT or mutant LAMB2/Gluc were evaluated by quantitative real-time PCR; 1 μ l cDNA was added to SYBR Green PCR Master Mix (Qiagen) and subjected to PCR amplification (one cycle at 95°C for 20 seconds and 40 cycles at 95°C for 1 second and 60°C for 20 seconds) in an Applied Biosystems 7900HT Fast Real-Time PCR System (Life Technologies, Grand Island, NY) using human β -actin as an internal control. Quantitative PCR was conducted in triplicate for each sample. The sequences of primers were LAMB2/Gluc forward: CATGGAG-CAGTTCATCGCAC, reverse: GTCAGAACACTGCACGTTGG; human β -actin forward: GGCACCCAGCACAAATGAAG, reverse: GGCACCCAGCACAAATGAAG.

ACKNOWLEDGMENTS

We thank Jeanette Cunningham for performing electron microscopy, Jennifer Richardson for genotyping mice, generous colleagues for antibodies, the Mouse Genetics Core and the Washington University Center for Kidney Disease Research (National Institutes of Health P30DK079333) for generation of transgenic mice and measuring urine protein and creatinine, and the Pulmonary Morphology Core (supported by National Institutes of Health P01HL029594) for histology.

Mice were housed in a facility supported by National Institutes of Health Grant C06RR015502. Y.M.C. was supported by National Institutes of Health Grants T32DK007126, K08DK089015, and P30DK079333 (Pilot and Feasibility Study). This research was supported by National Institutes of Health Grants R01DK078314 and R01GM060432 (to J.H.M.).

Part of this material was presented in abstract form at the 2012 Annual Meeting of the American Society of Nephrology, November 1–4, 2012, in San Diego, CA.

DISCLOSURES

None.

REFERENCES

- Zenker M, Tralau T, Lennert T, Pitz S, Mark K, Madlon H, Dötsch J, Reis A, Müntefering H, Neumann LM: Congenital nephrosis, mesangial sclerosis, and distinct eye abnormalities with microcoria: An autosomal recessive syndrome. *Am J Med Genet A* 130A: 138–145, 2004
- Zenker M, Pierson M, Jonveaux P, Reis A: Demonstration of two novel LAMB2 mutations in the original Pierson syndrome family reported 42 years ago. *Am J Med Genet A* 138: 73–74, 2005
- Matejas V, Hinkes B, Alkandari F, Al-Gazali L, Annestad E, Aytac MB, Barrow M, Bláhová K, Bockenbauer D, Cheong HI, Maruniak-Chudek I, Cochat P, Dötsch J, Gajjar P, Hennekam RC, Janssen F, Kagan M, Kariminejad A, Kemper MJ, Koenig J, Kogan J, Kroes HY, Kuwertz-Bröking E, Lewanda AF, Medeira A, Muscheites J, Niaudet P, Pierson M, Saggat A, Seaver L, Suri M, Tsygin A, Wühl E, Zurowska A, Uebe S, Hildebrandt F, Antignac C, Zenker M: Mutations in the human laminin beta2 (LAMB2) gene and the associated phenotypic spectrum. *Hum Mutat* 31: 992–1002, 2010
- Zenker M, Aigner T, Wendler O, Tralau T, Müntefering H, Fenski R, Pitz S, Schumacher V, Royer-Pokora B, Wühl E, Cochat P, Bouvier R, Kraus C, Mark K, Madlon H, Dötsch J, Rascher W, Maruniak-Chudek I, Lennert T, Neumann LM, Reis A: Human laminin beta2 deficiency causes congenital nephrosis with mesangial sclerosis and distinct eye abnormalities. *Hum Mol Genet* 13: 2625–2632, 2004
- Sasaki T, Fässler R, Hohenester E: Laminin: The crux of basement membrane assembly. *J Cell Biol* 164: 959–963, 2004
- Abrahamson DR: Origin of the glomerular basement membrane visualized after in vivo labeling of laminin in newborn rat kidneys. *J Cell Biol* 100: 1988–2000, 1985
- Miner JH, Yurchenco PD: Laminin functions in tissue morphogenesis. *Annu Rev Cell Dev Biol* 20: 255–284, 2004
- Aumailley M, Bruckner-Tuderman L, Carter WG, Deutzmann R, Edgar D, Ekblom P, Engel J, Engvall E, Hohenester E, Jones JCR, Kleinman HK, Marinkovich MP, Martin GR, Mayer U, Meneguzzi G, Miner JH, Miyazaki K, Patarroyo M, Paulsson M, Quaranta V, Sanes JR, Sasaki T, Sekiguchi K, Sorokin LM, Talts JF, Tryggvason K, Uitto J, Virtanen I, von der Mark K, Wewer UM, Yamada Y, Yurchenco PD: A simplified laminin nomenclature. *Matrix Biol* 24: 326–332, 2005
- Miner JH: Building the glomerulus: A matricentric view. *J Am Soc Nephrol* 16: 857–861, 2005
- Yurchenco PD, Cheng YS: Self-assembly and calcium-binding sites in laminin. A three-arm interaction model. *J Biol Chem* 268: 17286–17299, 1993
- Cheng YS, Champlaud MF, Burgeson RE, Marinkovich MP, Yurchenco PD: Self-assembly of laminin isoforms. *J Biol Chem* 272: 31525–31532, 1997
- Noakes PG, Miner JH, Gautam M, Cunningham JM, Sanes JR, Merlie JP: The renal glomerulus of mice lacking s-laminin/laminin beta 2: Nephrosis despite molecular compensation by laminin beta 1. *Nat Genet* 10: 400–406, 1995
- Knight D, Tolley LK, Kim DK, Lavidis NA, Noakes PG: Functional analysis of neurotransmission at beta2-laminin deficient terminals. *J Physiol* 546: 789–800, 2003
- Nishimune H, Sanes JR, Carlson SS: A synaptic laminin-calcium channel interaction organizes active zones in motor nerve terminals. *Nature* 432: 580–587, 2004
- Noakes PG, Gautam M, Mudd J, Sanes JR, Merlie JP: Aberrant differentiation of neuromuscular junctions in mice lacking s-laminin/laminin beta 2. *Nature* 374: 258–262, 1995
- Patton BL, Chiu AY, Sanes JR: Synaptic laminin prevents glial entry into the synaptic cleft. *Nature* 393: 698–701, 1998
- Libby RT, Lavallee CR, Balkema GW, Brunken WJ, Hunter DD: Disruption of laminin beta2 chain production causes alterations in morphology and function in the CNS. *J Neurosci* 19: 9399–9411, 1999
- Hasselbacher K, Wiggins RC, Matejas V, Hinkes BG, Mucha B, Hoskins BE, Ozaltin F, Nürnberg G, Becker C, Hangan D, Pohl M, Kuwertz-Bröking E, Griebel M, Schumacher V, Royer-Pokora B, Bakkaloglu A, Nürnberg P, Zenker M, Hildebrandt F: Recessive missense mutations in LAMB2 expand the clinical spectrum of LAMB2-associated disorders. *Kidney Int* 70: 1008–1012, 2006
- Chen YM, Kikkawa Y, Miner JH: A missense LAMB2 mutation causes congenital nephrotic syndrome by impairing laminin secretion. *J Am Soc Nephrol* 22: 849–858, 2011
- Dobson CM: Protein misfolding, evolution and disease. *Trends Biochem Sci* 24: 329–332, 1999

21. Sanders CR, Nagy JK: Misfolding of membrane proteins in health and disease: The lady or the tiger? *Curr Opin Struct Biol* 10: 438–442, 2000
22. Munro S, Pelham HR: An Hsp70-like protein in the ER: Identity with the 78 kd glucose-regulated protein and immunoglobulin heavy chain binding protein. *Cell* 46: 291–300, 1986
23. Ellgaard L, Helenius A: Quality control in the endoplasmic reticulum. *Nat Rev Mol Cell Biol* 4: 181–191, 2003
24. Ron D, Walter P: Signal integration in the endoplasmic reticulum unfolded protein response. *Nat Rev Mol Cell Biol* 8: 519–529, 2007
25. Harding HP, Novoa I, Zhang Y, Zeng H, Wek R, Schapira M, Ron D: Regulated translation initiation controls stress-induced gene expression in mammalian cells. *Mol Cell* 6: 1099–1108, 2000
26. Howard M, Welch WJ: Manipulating the folding pathway of delta F508 CFTR using chemical chaperones. *Methods Mol Med* 70: 267–275, 2002
27. Lomas DA, Evans DL, Finch JT, Carrell RW: The mechanism of Z alpha 1-antitrypsin accumulation in the liver. *Nature* 357: 605–607, 1992
28. Saliba RS, Munro PM, Luthert PJ, Cheetham ME: The cellular fate of mutant rhodopsin: Quality control, degradation and aggresome formation. *J Cell Sci* 115: 2907–2918, 2002
29. Koo EH, Lansbury PT Jr, Kelly JW: Amyloid diseases: Abnormal protein aggregation in neurodegeneration. *Proc Natl Acad Sci U S A* 96: 9989–9990, 1999
30. Inagi R: Endoplasmic reticulum stress in the kidney as a novel mediator of kidney injury. *Nephron, Exp Nephrol* 112: e1–e9, 2009
31. Miner JH, Go G, Cunningham J, Patton BL, Jarad G: Transgenic isolation of skeletal muscle and kidney defects in laminin beta2 mutant mice: Implications for Pierson syndrome. *Development* 133: 967–975, 2006
32. Abrahamson DR, Isom K, Roach E, Stroganova L, Zelenchuk A, Miner JH, St John PL: Laminin compensation in collagen alpha3(IV) knockout (Alport) glomeruli contributes to permeability defects. *J Am Soc Nephrol* 18: 2465–2472, 2007
33. Miner JH, Patton BL, Lentz SI, Gilbert DJ, Snider WD, Jenkins NA, Copeland NG, Sanes JR: The laminin alpha chains: Expression, developmental transitions, and chromosomal locations of alpha1-5, identification of heterotrimeric laminins 8-11, and cloning of a novel alpha3 isoform. *J Cell Biol* 137: 685–701, 1997
34. Miner JH, Sanes JR: Collagen IV α 3, α 4, and α 5 chains in rodent basal laminae: Sequence, distribution, association with laminins, and developmental switches. *J Cell Biol* 127: 879–891, 1994
35. Jarad G, Cunningham J, Shaw AS, Miner JH: Proteinuria precedes podocyte abnormalities in *Lamb2*^{-/-} mice, implicating the glomerular basement membrane as an albumin barrier. *J Clin Invest* 116: 2272–2279, 2006
36. Yoshida H: ER stress and diseases. *FEBS J* 274: 630–658, 2007
37. Schröder M, Kaufman RJ: The mammalian unfolded protein response. *Annu Rev Biochem* 74: 739–789, 2005
38. He F, Chen S, Wang H, Shao N, Tian X, Jiang H, Liu J, Zhu Z, Meng X, Zhang C: Regulation of CD2-associated protein influences podocyte endoplasmic reticulum stress-mediated apoptosis induced by albumin overload. *Gene* 484: 18–25, 2011
39. Hinkes BG, Mucha B, Vlangos CN, Gbadegesin R, Liu J, Hasselbacher K, Hangan D, Ozaltin F, Zenker M, Hildebrandt F; Arbeitsgemeinschaft für Paediatrische Nephrologie Study Group: Nephrotic syndrome in the first year of life: Two thirds of cases are caused by mutations in 4 genes (NPHS1, NPHS2, WT1, and LAMB2). *Pediatrics* 119: e907–e919, 2007
40. Cheng SH, Gregory RJ, Marshall J, Paul S, Souza DW, White GA, O’Riordan CR, Smith AE: Defective intracellular transport and processing of CFTR is the molecular basis of most cystic fibrosis. *Cell* 63: 827–834, 1990
41. Hofmann S, Bauer MF: Wolfram syndrome-associated mutations lead to instability and proteasomal degradation of wolframin. *FEBS Lett* 580: 4000–4004, 2006
42. Cohen FE, Kelly JW: Therapeutic approaches to protein-misfolding diseases. *Nature* 426: 905–909, 2003
43. Powell K, Zeitlin PL: Therapeutic approaches to repair defects in deltaF508 CFTR folding and cellular targeting. *Adv Drug Deliv Rev* 54: 1395–1408, 2002
44. Burrows JA, Willis LK, Perlmutter DH: Chemical chaperones mediate increased secretion of mutant alpha 1-antitrypsin (alpha 1-AT) Z: A potential pharmacological strategy for prevention of liver injury and emphysema in alpha 1-AT deficiency. *Proc Natl Acad Sci U S A* 97: 1796–1801, 2000
45. Morello JP, Salahpour A, Laperrière A, Bernier V, Arthus MF, Lonergan M, Petäjä-Repo U, Angers S, Morin D, Bichet DG, Bouvier M: Pharmacological chaperones rescue cell-surface expression and function of misfolded V2 vasopressin receptor mutants. *J Clin Invest* 105: 887–895, 2000
46. Sawkar AR, Cheng WC, Beutler E, Wong CH, Balch WE, Kelly JW: Chemical chaperones increase the cellular activity of N370S beta-glucosidase: A therapeutic strategy for Gaucher disease. *Proc Natl Acad Sci U S A* 99: 15428–15433, 2002
47. Fan JQ, Ishii S, Asano N, Suzuki Y: Accelerated transport and maturation of lysosomal alpha-galactosidase A in Fabry lymphoblasts by an enzyme inhibitor. *Nat Med* 5: 112–115, 1999
48. Sanes JR, Engvall E, Butkowski R, Hunter DD: Molecular heterogeneity of basal laminae: Isoforms of laminin and collagen IV at the neuromuscular junction and elsewhere. *J Cell Biol* 111: 1685–1699, 1990
49. Harvey SJ, Jarad G, Cunningham J, Rops AL, van der Vlag J, Berden JH, Moeller MJ, Holzman LB, Burgess RW, Miner JH: Disruption of glomerular basement membrane charge through podocyte-specific mutation of agrin does not alter glomerular permselectivity. *Am J Pathol* 171: 139–152, 2007
50. St John PL, Wang R, Yin Y, Miner JH, Robert B, Abrahamson DR: Glomerular laminin isoform transitions: Errors in metanephric culture are corrected by grafting. *Am J Physiol Renal Physiol* 280: F695–F705, 2001
51. Sasaki T, Mann K, Miner JH, Miosge N, Timpl R: Domain IV of mouse laminin beta1 and beta2 chains. *Eur J Biochem* 269: 431–442, 2002

This article contains supplemental material online at <http://jasn.asnjournals.org/lookup/suppl/doi:10.1681/ASN.2012121149/-/DCSupplemental>.